

Status of Exclusive Baryonic B Decays

Hai-Yang Cheng

Institute of Physics, Academia Sinica, Taipei, Taiwan 115, Republic of China

The status of exclusive two-body and three-body baryonic B decays is reviewed. The threshold peaking effect in baryon pair invariant mass is stressed and explained. Weak radiative baryonic B decays mediated by the electromagnetic penguin process are discussed.

PACS numbers: 13.25.Hw, 14.20.pt, 14.20.Lq

I. INTRODUCTION

A unique feature of hadronic B decays is that the B meson is heavy enough to allow a baryon-antibaryon pair production in the final state. During the Lepton-Photon Conference in 1987, ARGUS announced the first measurement of the decay modes $p\bar{p}\pi^\pm$ and $p\bar{p}\pi^+\pi^-$ in B decays at the level of 10^{-4} [1]. Although this observation of charmless baryonic B decays was immediately ruled out by CLEO [2], it nevertheless has stimulated extensive theoretical studies during the period of 1988-1992. Several different model frameworks have been proposed: the constituent quark model [3], the pole model [4, 5], the QCD sum rule [6], the diquark model [7] and flavor symmetry considerations [8].

However, experimental and theoretical activities in baryonic B decays suddenly faded away after 1992. This situation was dramatically changed in the past three years. Interest in this area was revived by many new measurements at CLEO and Belle followed by several theoretical studies.

A. Experimental status

two-body decays: Except for the recently measured $\bar{B}^0 \rightarrow \Lambda_c^+\bar{p}$ by Belle [9]

$$\mathcal{B}(\bar{B}^0 \rightarrow \Lambda_c^+\bar{p}) = (2.19_{-0.49}^{+0.56} \pm 0.32 \pm 0.57) \times 10^{-5}, (1)$$

none of the two-body baryonic B decays has been observed. The experimental upper limits are summarized in Tables I and III for charmless and charmful decays, respectively. We see that the present limit on charmless ones is generally of order 10^{-6} except for the $p\bar{p}$ mode which was recently pushed down to the level of 2.7×10^{-7} by BaBar [10].

three-body decays: Unlike the two-body case, the measurements of three-body or four-body baryonic B decays are quite fruitful and many new results have been emerged in recent years. For the charmless case, Belle [13] has observed 5 modes, see Table II. The channel $B^- \rightarrow p\bar{p}K^-$ announced by Belle nearly two years ago [14] is the first observation of charmless baryonic B decay.

Table III summarizes the measured branching ratios of charmful baryonic decays with a charmed meson or a charmed baryon in the final state. In general, Belle [15]

TABLE I: Experimental upper limits on the branching ratios of charmless two-body baryonic B decays.

Decay	CLEO [11]	Belle [12]	BaBar [10]
$\bar{B}^0 \rightarrow p\bar{p}$	1.4×10^{-6}	1.2×10^{-6}	2.7×10^{-7}
$\bar{B}^0 \rightarrow \Lambda\bar{\Lambda}$	1.2×10^{-6}	1.0×10^{-6}	
$B^- \rightarrow \Lambda\bar{p}$	1.5×10^{-6}	2.2×10^{-6}	
$B^- \rightarrow p\bar{\Delta}^{--}$	1.5×10^{-4}		
$B^- \rightarrow \Delta^0\bar{p}$	3.8×10^{-4}		
$\bar{B}^0 \rightarrow \Delta^{++}\Delta^{--}$	1.1×10^{-4}		
$\bar{B}^0 \rightarrow \Delta^0\bar{\Delta}^0$	1.5×10^{-3}		

TABLE II: Branching ratios of charmless three-body baryonic B decays measured by Belle [13].

Decay	Br(10^{-6})
$\bar{B}^0 \rightarrow \Lambda\bar{p}\pi^+$	$3.97_{-0.80}^{+1.00} \pm 0.56$
$B^- \rightarrow p\bar{p}K^-$	$5.66_{-0.57}^{+0.67} \pm 0.62$
$B^- \rightarrow p\bar{p}K^{*-}$	$10.3_{-2.8-1.7}^{+3.6+1.3}$
$\bar{B}^0 \rightarrow p\bar{p}K_S$	$1.88_{-0.60}^{+0.77} \pm 0.23$
$B^- \rightarrow p\bar{p}\pi^-$	$3.06_{-0.62}^{+0.73} \pm 0.37$
$\bar{B}^0 \rightarrow \Lambda\bar{p}K^+$	< 0.82
$\bar{B}^0 \rightarrow \Sigma^0\bar{p}\pi^+$	< 3.8

and CLEO [16] results are consistent with each other except for the ratio of $\Sigma_c^{++}\bar{p}\pi^-$ to $\Sigma_c^0\bar{p}\pi^+$. The Σ_c^{++} decay proceeds via both external and internal W -emission diagrams, whereas the Σ_c^0 decay can only proceed via an internal W emission. While Belle measurements imply a sizable suppression for the Σ_c^0 decay (and likewise for the Σ_{c1} decay), it is found by CLEO that $\Sigma_c^{++}\bar{p}\pi^-$, $\Sigma_c^0\bar{p}\pi^+$ and $\Sigma_c^0\bar{p}\pi^0$ are of the same order of magnitude. Therefore, it is concluded by CLEO that the external W decay diagram does not dominate over the internal W -emission diagram in Cabibbo-allowed baryonic B decays. This needs to be clarified by the forthcoming improved measurements. The decay $B^- \rightarrow J/\psi\Lambda\bar{p}$ was recently measured by BaBar with the branching ratio $(12_{-6}^{+9}) \times 10^{-6}$ [17] and an upper limit 4.1×10^{-5} was set by Belle [18].

A common and unique feature of the spectrum for $B \rightarrow \mathcal{B}_1\bar{\mathcal{B}}_2M$ (e.g. $\bar{B}^0 \rightarrow \Lambda\bar{p}\pi^+$) is the threshold enhancement behavior of the baryon-pair invariant mass (see Fig. 1): It sharply peaks at very low values. That is, the B meson is preferred to decay into a baryon-antibaryon pair with

TABLE III: Experimental measurements of the branching ratios (in units of 10^{-4}) for the B decay modes with a charmed baryon Λ_c or $\Lambda_{c1} = \Lambda_c(2593), \Lambda_c(2625)$ or $\Sigma_c(2455)$ or $\Sigma_{c1} = \Sigma_c(2520)$ or a charmed meson in the final state.

Mode	Belle [9, 15]	CLEO [16]
$B^- \rightarrow \Lambda_c^+ \bar{p} \pi^- \pi^0$		$18.1 \pm 2.9_{-1.6}^{+2.2} \pm 4.7$
$\bar{B}^0 \rightarrow \Lambda_c^+ \bar{p} \pi^+ \pi^-$	$11.0 \pm 1.2 \pm 1.9 \pm 2.9$	$16.7 \pm 1.9_{-1.6}^{+1.9} \pm 4.3$
$B^- \rightarrow \Lambda_c^+ \bar{p} \pi^-$	$1.87_{-0.40}^{+0.43} \pm 0.28 \pm 0.49$	$2.4 \pm 0.6_{-0.17}^{+0.19} \pm 0.6$
$\bar{B}^0 \rightarrow \Lambda_c^+ \bar{p}$	$0.22_{-0.05}^{+0.06} \pm 0.03 \pm 0.06$	< 0.9
$B^- \rightarrow \Lambda_{c1}^+ \bar{p} \pi^-$		< 1.9
$\bar{B}^0 \rightarrow \Lambda_{c1}^+ \bar{p}$		< 1.1
$B^- \rightarrow \Sigma_c^{++} \bar{p} \pi^- \pi^-$		$2.8 \pm 0.9 \pm 0.5 \pm 0.7$
$B^- \rightarrow \Sigma_c^0 \bar{p} \pi^+ \pi^-$		$4.4 \pm 1.2 \pm 0.5 \pm 1.1$
$\bar{B}^0 \rightarrow \Sigma_c^{++} \bar{p} \pi^-$	$2.38_{-0.55}^{+0.63} \pm 0.41 \pm 0.62$	$3.7 \pm 0.8 \pm 0.7 \pm 0.8$
$\bar{B}^0 \rightarrow \Sigma_c^0 \bar{p} \pi^+$	$0.84_{-0.35}^{+0.42} \pm 0.14 \pm 0.22 < 1.59$	$2.2 \pm 0.6 \pm 0.4 \pm 0.5$
$B^- \rightarrow \Sigma_c^0 \bar{p} \pi^0$		$4.2 \pm 1.3 \pm 0.4 \pm 1.0$
$B^- \rightarrow \Sigma_c^0 \bar{p}$	$0.45_{-0.19}^{+0.26} \pm 0.07 \pm 0.12 < 0.93$	< 0.8
$\bar{B}^0 \rightarrow \Sigma_{c1}^{++} \bar{p} \pi^-$	$1.63_{-0.51}^{+0.57} \pm 0.28 \pm 0.42$	
$\bar{B}^0 \rightarrow \Sigma_{c1}^0 \bar{p} \pi^+$	$0.48_{-0.40}^{+0.45} \pm 0.08 \pm 0.12 < 1.21$	
$B^- \rightarrow \Sigma_{c1}^0 \bar{p}$	$0.14_{-0.09}^{+0.15} \pm 0.02 \pm 0.04 < 0.46$	
$\bar{B}^0 \rightarrow D^{*+} n \bar{p}$		$14.5_{-3.0}^{+3.4} \pm 2.7$
$\bar{B}^0 \rightarrow D^0 p \bar{p}$	$1.18 \pm 0.15 \pm 0.16$	
$\bar{B}^0 \rightarrow D^{*0} p \bar{p}$	$1.20_{-0.29}^{+0.33} \pm 0.21$	

low invariant mass accompanied by a fast recoil meson.

B. Theoretical progress

Since baryonic B decays involve two baryons, it is extremely complicated and much involved. Nevertheless, there are some theoretical progresses in the past three years.

It is known that two-body baryonic B decays are dominated by nonfactorizable contributions that are difficult to evaluate. This nonfactorizable effect can be evaluated in the pole model. Using the MIT bag model to evaluate the weak matrix elements and the 3P_1 model to estimate the strong coupling constants, it is found in [19] and [20] that the charmless and charmful two-body decays can be well described. Chang and Hou [21] have generalized the original version of the diquark model in [7] to include penguin effects, but no quantitative predictions have been made. In the past year, a diagrammatic approach has been developed for both charmful [22] and charmless [23] decays.

As pointed out by Dunietz [24] and by Hou and Soni [25], the smallness of the two-body baryonic decay $B \rightarrow \mathcal{B}_1 \bar{\mathcal{B}}_2$ has to do with a straightforward Dalitz plot analysis or with the large energy release. Hou and Soni conjectured that in order to have larger baryonic B decays, one has to reduce the energy release and at the same time allow for baryonic ingredients to be present in the final state. This is indeed the near threshold effect mentioned before. Of course, one has to understand the underlying origin of the threshold peaking effect.

Contrary to the two-body baryonic B decay, the three-body decays do receive factorizable contributions that fall into two categories: (i) the transition process with a meson emission, $\langle M | (\bar{q}_3 q_2) | 0 \rangle \langle \mathcal{B}_1 \bar{\mathcal{B}}_2 | (\bar{q}_1 b) | B \rangle$, and (ii) the

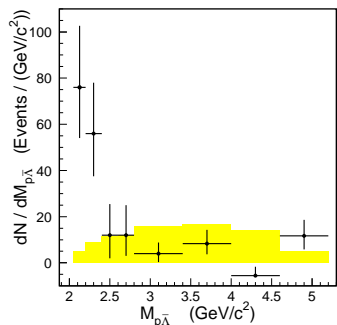


FIG. 1: The $p\bar{\Lambda}$ invariant mass distribution of $B^0 \rightarrow \bar{\Lambda} p \pi^-$ [13].

Now it is well established experimentally that

$$\begin{aligned}
 \mathcal{B}(B^- \rightarrow \Lambda_c^+ \bar{p} \pi^-) &\gg \mathcal{B}(\bar{B}^0 \rightarrow \Lambda_c^+ \bar{p}), \\
 \mathcal{B}(B^- \rightarrow p \bar{p} K^-) &\gg \mathcal{B}(\bar{B}^0 \rightarrow p \bar{p}), \\
 \mathcal{B}(B^- \rightarrow \Sigma_c^0 \bar{p} \pi^0) &\gg \mathcal{B}(B^- \rightarrow \Sigma_c^0 \bar{p}). \quad (2)
 \end{aligned}$$

Therefore, some three-body final states have rates larger than their two-body counterparts. This phenomenon can be understood in terms of the threshold effect, namely, the invariant mass of the baryon pair is preferred to be close to the threshold. The configuration of the two-body decay $B \rightarrow \mathcal{B}_1 \bar{\mathcal{B}}_2$ is not favorable since its invariant mass is m_B . In $B \rightarrow \mathcal{B}_1 \bar{\mathcal{B}}_2 M$ decays, the effective mass of the baryon pair is reduced as the emitted meson can carry away much energies.

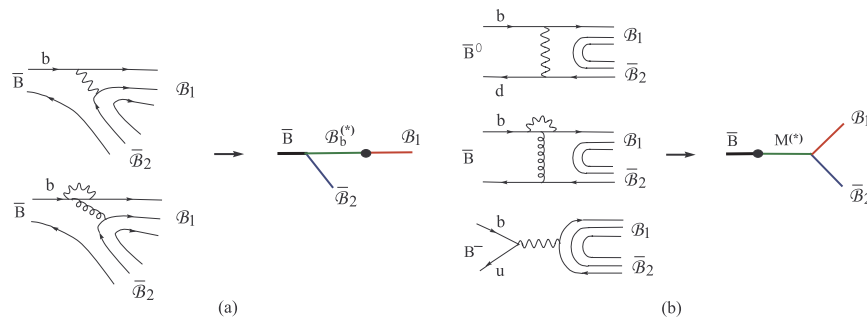


FIG. 2: Quark and pole diagrams for two-body baryonic B decay $\bar{B} \rightarrow \mathcal{B}_1 \bar{\mathcal{B}}_2$, where the symbol \bullet denotes the weak vertex.

current-induced process governed by the factorizable amplitude $\langle \mathcal{B}_1 \bar{\mathcal{B}}_2 | (\bar{q}_1 q_2) | 0 \rangle \langle M | (\bar{q}_3 b) | B \rangle$. The two-body matrix element $\langle \mathcal{B}_1 \bar{\mathcal{B}}_2 | (\bar{q}_1 q_2) | 0 \rangle$ in the latter process can be either related to some measurable quantities or calculated using the quark model. The current-induced contribution to three-body baryonic B decays has been discussed in various publications [26, 27, 28]. On the contrary, it is difficult to evaluate the three-body matrix element in the transition process and in this case one can appeal to the pole model [19, 20, 29].

Weak radiative baryonic B decays $B \rightarrow \mathcal{B}_1 \bar{\mathcal{B}}_2 \gamma$ mediated by the electromagnetic penguin process $b \rightarrow s \gamma$ may have appreciable rates. Based on the pole model, it is found that $B^- \rightarrow \Lambda \bar{p} \gamma$ and $B^- \rightarrow \Xi^0 \bar{\Sigma}^- \gamma$ have sizable rates and are readily accessible [30].

II. 2-BODY BARYONIC B DECAYS

As shown in Fig. 2, the quark diagrams for two-body baryonic B decays consist of internal W -emission diagram, $b \rightarrow d(s)$ penguin transition, W -exchange for the neutral B meson and W -annihilation for the charged B . Just as mesonic B decays, W -exchange and W -annihilation are expected to be helicity suppressed and the former is furthermore subject to color suppression. Therefore, the two-body baryonic B decay $B \rightarrow \mathcal{B}_1 \bar{\mathcal{B}}_2$ receives the main contributions from the internal W -emission diagram for tree-dominated modes and the penguin diagram for penguin-dominated processes.

These amplitudes are nonfactorizable in nature and thus very difficult to evaluate directly. In order to circumvent this difficulty, it is customary to assume that the decay amplitude at the hadron level is dominated by the pole diagrams with low-lying one-particle intermediate states. The general amplitude reads

$$\mathcal{A}(B \rightarrow \mathcal{B}_1 \bar{\mathcal{B}}_2) = \bar{u}_1 (A + B \gamma_5) v_2, \quad (3)$$

where A and B correspond to p -wave parity-violating (PV) and s -wave parity-conserving (PC) amplitudes, respectively. In the pole model, PC and PV amplitudes are dominated by $\frac{1}{2}^+$ ground-state intermediate states and $\frac{1}{2}^-$ low-lying baryon resonances, respectively. This

pole model has been applied successfully to nonleptonic decays of hyperons and charmed baryons [31, 32]. In general, the pole diagram leads to

$$A = - \sum_{\mathcal{B}_b^*} \frac{g_{\mathcal{B}_b^* \rightarrow B \mathcal{B}_2} b_{\mathcal{B}_b^* \mathcal{B}_1}}{m_1 - m_{\mathcal{B}_b^*}}, \quad B = \sum_{\mathcal{B}_b} \frac{g_{\mathcal{B}_b \rightarrow B \mathcal{B}_2} a_{\mathcal{B}_b \mathcal{B}_1}}{m_1 - m_{\mathcal{B}_b}}. \quad (4)$$

There are two unknown quantities in the above equation: weak matrix elements and strong couplings. For the former we employ the MIT bag model to evaluate the baryon-to-baryon transitions [19]. For the latter, there are two distinct models for quark pair creation: (i) the 3P_0 model in which the $q\bar{q}$ pair is created from the vacuum with vacuum quantum numbers. Presumably it works in the nonperturbative low energy regime, and (ii) the 3S_1 model in which the quark pair is created perturbatively via one gluon exchange with one-gluon quantum numbers 3S_1 . Since the light baryons produced in two-body baryonic B decays are very energetic, it appears that the 3S_1 model may be more relevant.

TABLE IV: Predictions of charmful two-body baryonic B decays. Experimental results are taken from Table III.

	[5]	[20]	Expt.
$\bar{B}^0 \rightarrow \Lambda_c^+ \bar{p}$	1.1×10^{-3}	1.1×10^{-5}	$(2.19 \pm 0.84) \times 10^{-5}$
$B^- \rightarrow \Sigma_c^0 \bar{p}$	1.5×10^{-2}	6.0×10^{-5}	$< 8.0 \times 10^{-5}$
$\bar{B}^0 \rightarrow \Sigma_c^0 \bar{n}$	5.8×10^{-3}	6.0×10^{-7}	
$B^- \rightarrow \Lambda_c^+ \bar{\Delta}^{--}$	3.6×10^{-2}	1.9×10^{-5}	

The predictions for charmful $B \rightarrow \mathcal{B}_1 \bar{\mathcal{B}}_2$ decays are summarized in Table IV. All earlier predictions based on the sum-rule analysis, the pole model and the diquark model are too large compared to experiment. Note that we predict that $B^- \rightarrow \Sigma_c^0 \bar{p}$ has a larger rate than $\bar{B}^0 \rightarrow \Lambda_c \bar{p}$ since the former proceeds via the Λ_b pole while the latter via Σ_b pole and the $\Lambda_b N \bar{B}$ coupling is larger than $\Sigma_b N \bar{B}$ [20]. Therefore, it is important to measure the $\Sigma_c^0 \bar{p}$ production to test the pole model.

From Table V we see that the charmless two-body baryonic decays are predicted at the level of 10^{-7} . This is consistent with the observation of $\bar{B}^0 \rightarrow \Lambda_c^+ \bar{p}$ after a simple scaling of $|V_{ub}/V_{cb}|^2$.

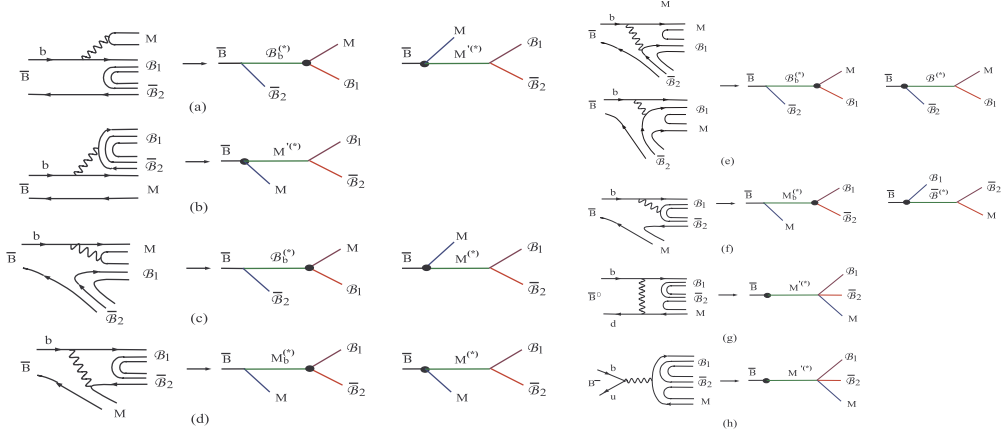


FIG. 3: Quark and pole diagrams for three-body baryonic B decay $\bar{B} \rightarrow \mathcal{B}_1 \bar{\mathcal{B}}_2 M$, where the symbol \bullet denotes the weak vertex.

TABLE V: Predictions of the branching ratios for some charmless two-body baryonic B decays classified into two categories: tree-dominated and penguin-dominated. Branching ratios denoted by “†” are calculated only for the parity-conserving part. Experimental limits are taken from Table I.

	[6]	[5]	[19]	Expt.
$\bar{B}^0 \rightarrow p\bar{p}$	1.2×10^{-6}	7.0×10^{-6}	$1.1 \times 10^{-7\dagger}$	$< 2.7 \times 10^{-6}$
$\bar{B}^0 \rightarrow n\bar{n}$	3.5×10^{-7}	7.0×10^{-6}	$1.2 \times 10^{-7\dagger}$	
$B^- \rightarrow n\bar{p}$	6.9×10^{-7}	1.7×10^{-5}	5.0×10^{-7}	
$\bar{B}^0 \rightarrow \Lambda\bar{\Lambda}$		2×10^{-7}	0^\dagger	$< 1.0 \times 10^{-6}$
$B^- \rightarrow p\bar{\Delta}^{--}$	2.9×10^{-7}	3.2×10^{-4}	1.4×10^{-6}	$< 1.5 \times 10^{-4}$
$\bar{B}^0 \rightarrow p\bar{\Delta}^-$	7×10^{-8}	1.0×10^{-4}	4.3×10^{-7}	
$B^- \rightarrow n\bar{\Delta}^-$		1×10^{-7}	4.6×10^{-7}	
$\bar{B}^0 \rightarrow n\bar{\Delta}^0$		1.0×10^{-4}	4.3×10^{-7}	
$B^- \rightarrow \Lambda\bar{p}$	$\lesssim 3 \times 10^{-6}$		$2.2 \times 10^{-7\dagger}$	$< 1.5 \times 10^{-6}$
$\bar{B}^0 \rightarrow \Lambda\bar{n}$			$2.1 \times 10^{-7\dagger}$	
$\bar{B}^0 \rightarrow \Sigma^+\bar{p}$	6×10^{-6}		$1.8 \times 10^{-8\dagger}$	
$B^- \rightarrow \Sigma^0\bar{p}$	3×10^{-6}		$5.8 \times 10^{-8\dagger}$	
$B^- \rightarrow \Sigma^+\bar{\Delta}^{--}$	6×10^{-6}		2.0×10^{-7}	
$\bar{B}^0 \rightarrow \Sigma^+\bar{\Delta}^-$	6×10^{-6}		6.3×10^{-8}	
$B^- \rightarrow \Sigma^-\bar{\Delta}^0$	2×10^{-6}		8.7×10^{-8}	

III. 3-BODY BARYONIC B DECAYS

In the three-body baryonic decay, the emission of the meson M will carry away energies in such a way that the invariant mass of $\mathcal{B}_1 \bar{\mathcal{B}}_2$ becomes smaller and hence it is relatively easier to fragment into the baryon-antibaryon pair. One can also understand this feature more concretely by studying the Dalitz plot. Due to the $V - A$ nature of the $b \rightarrow ud\bar{u}$ process, the invariant mass of the diquark ud peaks at the highest possible values in a Dalitz plot for $b \rightarrow ud\bar{d}$ transition [33]. If the ud forms a nucleon, then the very massive udq objects will intend to form a highly excited baryon state such as Δ and N^* and will be seen as $Nn\pi$ ($n \geq 1$) [24]. This explains the non-

observation of the $N\bar{N}$ final states and why the three-body mode $N\bar{N}\pi(\rho)$ is favored. Of course, this argument is applicable only to the tree-dominated processes.

The quark diagrams and the corresponding pole diagrams for decays of B mesons to the baryonic final state $\mathcal{B}_1 \bar{\mathcal{B}}_2 M$ are more complicated. In general there are two external W -diagrams Figs. 3(a)-3(b), four internal W -emissions Figs. 3(c)-3(f), and one W -exchange Fig. 3(g) for the neutral B meson and one W -annihilation Fig. 3(h) for the charged B . Because of space limitation, penguin diagrams are not drawn in Fig. 3; they can be obtained from Figs. 3(c)-3(g) by replacing the $b \rightarrow u$ tree transition by the $b \rightarrow s(d)$ penguin transition. Under the factorization hypothesis, the relevant factorizable amplitudes are proportional to $\langle M | (\bar{q}_3 q_2) | 0 \rangle \langle \mathcal{B}_1 \bar{\mathcal{B}}_2 | (\bar{q}_1 b) | B \rangle$ for Figs. 3(a) and 3(c), and to $\langle \mathcal{B}_1 \bar{\mathcal{B}}_2 | (\bar{q}_1 q_2) | 0 \rangle \langle M | (\bar{q}_3 b) | B \rangle$ for Figs. 3(b) and 3(d). For Figs. 3(b) and 3(d) the two-body matrix element $\langle \mathcal{B}_1 \bar{\mathcal{B}}_2 | (\bar{q}_1 q_2) | 0 \rangle$ for octet baryons can be related to the e.m. form factors of the nucleon. For Figs. 3(a) and 3(c) we will consider the pole diagrams to evaluate 3-body matrix elements. The 3-body matrix element $\langle \mathcal{B}_1 \bar{\mathcal{B}}_2 | (\bar{q}_1 b) | B \rangle$ receives contributions from point-like contact interaction (i.e. direct weak transition) and pole diagrams [19].

We consider the decay $B^- \rightarrow \Lambda_c^+ \bar{p} \pi^-$ as an illustration. It receives resonant and nonresonant contributions. The factorizable nonresonant amplitude reads

$$\begin{aligned}
 A(B^- \rightarrow \Lambda_c^+ \bar{p} \pi^-)_{\text{fact}} &= \frac{G_F}{\sqrt{2}} V_{cb} V_{ud}^* \left\{ a_1 \langle \pi^- | (\bar{d}u) | 0 \rangle \right. \\
 &\quad \times \langle \Lambda_c^+ \bar{p} | (\bar{c}b) | B^- \rangle \\
 &\quad \left. + a_2 \langle \pi^- | (\bar{d}b) | B^- \rangle \langle \Lambda_c^+ \bar{p} | (\bar{c}u) | 0 \rangle \right\} \\
 &\equiv A_1 + A_2. \tag{5}
 \end{aligned}$$

The factorizable amplitude A_2 can be directly calculated [20]. For the amplitude A_1 we evaluate the baryon and meson pole diagrams in Fig. 4. Let's consider the baryon pole due to Λ_b in Fig. 4(a) whose propagator is given by $1/(m_{\Lambda_b}^2 - m_{\Lambda_c}^2 \pi)$. In the heavy quark limit, this propaga-

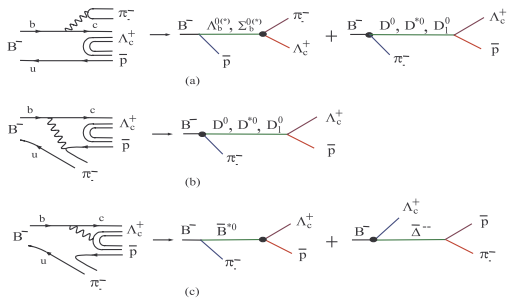


FIG. 4: Quark and pole diagrams for $B^- \rightarrow \Lambda_c^+ \bar{p} \pi^-$, where the solid blob denotes the weak vertex. (a) and (b) correspond to factorizable external and internal W -emission contributions, respectively, while (c) to nonfactorizable internal W -emission diagrams.

tor is not $1/m_b^2$ suppressed at the region where the invariant mass of $\Lambda_c \pi$ pair is large, for example, when the pion carries away much energies. For the meson poles in Figs. 4(a) and 4(b), the D meson propagator $1/(m_D^2 - m_{\Lambda_c \bar{p}}^2)$ is enhanced when the invariant mass of $\Lambda_c \bar{p}$ is near the threshold. This is equivalent to the $\Lambda_c \bar{p}$ form factor suppression at large momentum transfer. Therefore, as far as the factorizable diagrams Figs. 4(a) and 4(b) are concerned, the most favorable configuration is that the effective mass of $\Lambda_c \bar{p}$ is at its lowest value. It should be stressed that this configuration is not favored in Fig. 4(c). However, the latter contribution is nonfactorizable and hence it is presumably suppressed. Note that the measured spectrum can be used to constrain the momentum dependence of baryon-pair form factors.

The pole diagram of Fig. 2(a) for two-body decays is always $1/m_b^2$ suppressed and this explains why the three-body baryonic B decays can have rates larger than their two-body counterparts.

Many of 3-body baryonic B decays have been studied in [19, 20, 26, 27, 28, 29]. Because of space limitation, we will focus on a few of the prominent features of them:

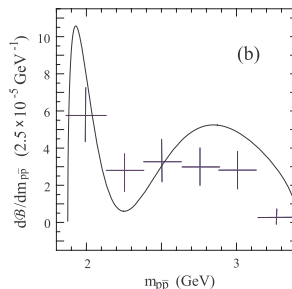
- About 1/4 of the $B^- \rightarrow \Lambda_c^+ \bar{p} \pi^-$ rate comes from resonant contributions [20].
- Contrary to $\bar{B}^0 \rightarrow D^{(*)+} n \bar{p}$ decays where the D^{*+}/D^+ production ratio is anticipated to be of order 3, the D^{*0}/D^0 production ratio in color suppressed $\bar{B}^0 \rightarrow D^{(*)0} p \bar{p}$ decays is consistent with unity experimentally (see Table III). It is shown in [29] that the similar rates for $D^0 p \bar{p}$ and $D^{*0} p \bar{p}$ can be understood within the framework of the pole model as the former is dominated by the axial-vector meson states, whereas the other modes proceed mainly through the vector meson poles.
- The spectrum of $B \rightarrow D^0 p \bar{p}$ is predicted to have a hump at large $p \bar{p}$ invariant mass $m_{p \bar{p}} \sim 2.9$ GeV [29] (see Fig. 5), which needs to be confirmed by forthcoming experiments.

- Charmless decays $B^- \rightarrow p \bar{p} K^- (K^{*-})$ are penguin-dominated and have the branching ratios

$$\begin{aligned} \mathcal{B}(B^- \rightarrow p \bar{p} K^-) &\approx 4.0 \times 10^{-6}, \\ \mathcal{B}(B^- \rightarrow p \bar{p} K^{*-}) &\approx 2.3 \times 10^{-6}, \end{aligned} \quad (6)$$

predicted by the pole model [19]. It is naively expected that $p \bar{p} K^{*-} < p \bar{p} K^-$ due to the absence of a_6 and a_8 penguin terms to the former. The Belle observation of a large rate for the K^* production (see Table II) is thus unexpected. Also, it is non-trivial to understand the observed sizable rate of $\bar{B}^0 \rightarrow p \bar{p} \bar{K}^0$ [19, 28].

- The decay $B \rightarrow \Lambda \bar{p} \pi$ was previously argued to be small ($< 10^{-6}$) and suppressed relative to $\Sigma^0 \bar{p} \pi^+$ [19]. The sizable branching ratio of the former $\sim 4.0 \times 10^{-6}$ observed recently by Belle [13] can be understood now as a proper treatment of the pseudoscalar form factor arising from penguin matrix elements [28].



IV. RADIATIVE BARYONIC B DECAYS

Naively it appears that the bremsstrahlung process will lead to $\Gamma(B \rightarrow \mathcal{B}_1 \bar{\mathcal{B}}_2 \gamma) \sim \mathcal{O}(\alpha_{\text{em}}) \Gamma(B \rightarrow \mathcal{B}_1 \bar{\mathcal{B}}_2)$ with α_{em} being an electromagnetic fine-structure constant and hence the radiative baryonic B decay is further suppressed than the two-body counterpart, making its observation very difficult at the present level of sensitivity for B factories. However, there is an important short-distance electromagnetic penguin transition $b \rightarrow s \gamma$. Owing to the large top quark mass, the amplitude of $b \rightarrow s \gamma$ is neither quark mixing nor loop suppressed. Moreover, it is largely enhanced by QCD corrections. As a consequence, the short-distance contribution due to the electromagnetic penguin diagram dominates over the bremsstrahlung. This phenomenon is quite unique to the bottom hadrons which contain a heavy b quark; such a magic short-distance enhancement does not occur in the systems of charmed and strange hadrons.

Consider the Λ_b pole diagram and apply heavy quark spin symmetry and static b quark limit to relate the tensor matrix element appearing in

$$\langle \Lambda(p_\Lambda) \gamma(\varepsilon, k) | \mathcal{H}_W | \Lambda_b(p_{\Lambda_b}) \rangle = -i \frac{G_F}{\sqrt{2}} \frac{e}{8\pi^2} V_{ts}^* V_{tb} \\ \times 2c_7^{\text{eff}} m_b \varepsilon^\mu k^\nu \langle \Lambda | \bar{s} \sigma_{\mu\nu} (1 + \gamma_5) b | \Lambda_b \rangle \quad (7)$$

to the $\Lambda_b \rightarrow \Lambda$ form factors. The decay rate depends on the strong coupling of $\Lambda_b B^+ \bar{p}$ and $\Lambda_b \rightarrow \Lambda$ transition form factors [30] and it is found [35]:

$$\mathcal{B}(B^- \rightarrow \Lambda \bar{p} \gamma) \approx \mathcal{B}(B^- \rightarrow \Xi^0 \bar{\Sigma}^- \gamma) \\ \sim 1.2 \times 10^{-6}. \quad (8)$$

Therefore, penguin-induced radiative baryonic B decay modes should be readily accessible by B factories. Recently, CLEO [34] has made the first attempt of measuring radiative baryonic B decays:

$$[\mathcal{B}(B^- \rightarrow \Lambda \bar{p} \gamma) + 0.3\mathcal{B}(B^- \rightarrow \Sigma^0 \bar{p} \gamma)]_{E_\gamma > 2.0 \text{ GeV}} \\ < 3.3 \times 10^{-6}. \quad (9)$$

Theoretically, the production of $\Sigma^0 \bar{p} \gamma$ is suppressed relative to $\Lambda \bar{p} \gamma$ [30].

V. CONCLUSION

Experimental and theoretical progresses in exclusive baryonic B decays in the past few years are impressive. The threshold peaking effect in baryon pair invariant mass is a key ingredient in understanding three-body decays. The weak radiative baryonic decays $B^- \rightarrow \Lambda \bar{p} \gamma$ and $B^- \rightarrow \Xi^0 \bar{\Sigma}^- \gamma$ mediated by the electromagnetic penguin process $b \rightarrow s \gamma$ have branching ratios of order 10^{-6} and should be readily accessible experimentally.

Acknowledgments

I wish to thank Kwei-Chou Yang for collaboration and Eung-Jin Chun for organizing this wonderful conference.

-
- [1] ARGUS Collaboration, H. Albrecht, Phys. Lett. B **209**, 119 (1988).
[2] CLEO Collaboration, C. Bebek *et al.*, Phys. Rev. Lett. **62**, 2436 (1989).
[3] J.G. Körner, Z. Phys. C **43**, 165 (1989).
[4] N.G. Deshpande, J. Trampetic, and A. Soni, Mod. Phys. Lett. A **3**, 749 (1988).
[5] M. Jarfi *et al.*, Phys. Rev. D **43**, 1599 (1991); Phys. Lett. B **237**, 513 (1990).
[6] V. Chernyak and I. Zhitnitsky, Nucl. Phys. B **345**, 137 (1990).
[7] P. Ball and H.G. Dosch, Z. Phys. C **51**, 445 (1991).
[8] M. Gronau and J.L. Rosner, Phys. Rev. D **37**, 688 (1988); G. Eilam, M. Gronau, and J.L. Rosner, *ibid.* **39**, 819 (1989); X.G. He, B.H.J. McKellar, and D.d. Wu, *ibid.* **41**, 2141 (1990); S.M. Sheikholeslami and M.P. Khanna, *ibid.* **44**, 770 (1991); S.M. Sheikholeslami, G.K. Sindana, and M.P. Khanna, Int. J. Mod. Phys. A **7**, 1111 (1992).
[9] Belle Collaboration, N. Gabyshev *et al.*, Phys. Rev. Lett. **90**, 121802 (2003).
[10] Talk presented by J. Fry at the XXI International Symposium on Lepton and Photon Interactions at High Energies, Fermilab, Aug. 11-16, 2003.
[11] CLEO Collaboration, A. Bornheim *et al.*, Phys. Rev. D **68**, 052002 (2003); T.E. Coan *et al.*, *ibid.* **59**, 111101 (1999).
[12] Belle Collaboration, K. Abe *et al.*, Phys. Rev. D **65**, 091103 (2002).
[13] Belle Collaboration, M.Z. Wang *et al.*, Phys. Rev. Lett. **90**, 201802 (2003); hep-ex/0310018.
[14] Belle Collaboration, K. Abe *et al.*, Phys. Rev. Lett. **88**, 181803 (2002).
[15] Belle Collaboration, N. Gabyshev *et al.*, Phys. Rev. D **66**, 091102 (2002); K. Abe *et al.*, Phys. Rev. Lett. **89**, 151802 (2002).
[16] CLEO Collaboration, S.A. Dytman *et al.*, Phys. Rev. D **66**, 091101 (2002); S. Anderson *et al.*, Phys. Rev. Lett. **86**, 2732 (2001).
[17] BaBar Collaboration, B. Aubert *et al.*, Phys. Rev. Lett. **90**, 231801 (2003).
[18] Belle Collaboration, S.L. Zang *et al.*, hep-ex/0309060.
[19] H.Y. Cheng and K.C. Yang, Phys. Rev. D **66**, 014020 (2002).
[20] H.Y. Cheng and K.C. Yang, Phys. Rev. D **67**, 034008 (2003); *ibid.* **65**, 054028 (2002).
[21] C.H. Chang and W.S. Hou, Eur. Phys. J. C **23**, 691 (2002).
[22] Z. Luo and J.L. Rosner, Phys. Rev. D **67**, 094017 (2003).
[23] C.K. Chua, Phys. Rev. D **68**, 074001 (2003).
[24] I. Dunietz, Phys. Rev. D **58**, 094010 (1998).
[25] W.S. Hou and A. Soni, Phys. Rev. Lett. **86**, 4247 (2001).
[26] C.K. Chua, W.S. Hou, and S.Y. Tsai, Phys. Rev. D **65**, 034003 (2002); Phys. Lett. B **528**, 233 (2002).
[27] C.K. Chua, W.S. Hou, and S.Y. Tsai, Phys. Rev. D **66**, 054004 (2002).
[28] C.K. Chua and W.S. Hou, Eur. Phys. J. C **29**, 27 (2003).
[29] H.Y. Cheng and K.C. Yang, Phys. Rev. D **66**, 094009 (2002).
[30] H.Y. Cheng and K.C. Yang, Phys. Lett. B **533**, 271 (2002).
[31] H.Y. Cheng and B. Tseng, Phys. Rev. D **46**, 1042 (1992); **55**, 1697(E) (1997).
[32] H.Y. Cheng and B. Tseng, Phys. Rev. D **48**, 4188 (1993).
[33] G. Buchalla, I. Dunietz, and H. Yamamoto, Phys. Lett. B **364**, 188 (1995).
[34] CLEO Collaboration, K.W. Edwards *et al.*, Phys. Rev. D **68**, 011102 (2003).
[35] The prediction of $B^- \rightarrow \Lambda \bar{p} \gamma$ in [30] is updated here using the strong coupling constants constrained from the measured 3-body charmful baryonic B decays.